RSC Advances

ROYAL SOCIETY OF CHEMISTRY

www.rsc.org/advances

Rapid fabrication of paper-based microfluidic analytical devices with desktop stereolithography 3D printer

Yong He[1,2] , Wen-bin Wu[1,2], Jian-zhong Fu[1,2]*

(1. The State Key Lab of Fluid Power Transmission and Control Systems, Department of Mechanical Engineering, Zhejiang University, Hangzhou 310027, China

2. Zhejiang Province's Key Laboratory of 3D Printing Process and Equipment, Department of Mechanical Engineering, Zhejiang University, Hangzhou 310027, China

Correspondence to Jiang-zhong Fu; e-mail: fjz@zju.edu.cn)

ABSTRACT

In this study, we developed a novel and facile method for fabricating paper-based microfluidic analytical devices (μPADs) with dynamic mask photo curing (DMPC), generated by a desktop stereolithography (SL) three-dimensional printer (3DP). First, we immersed filter paper in ultraviolet (UV) resin to cover it evenly. Next, we exposed it to UV-lights through a dynamic mask of the negative channel pattern. After curing, the UV-exposed regions become highly hydrophobic, creating hydrophobic barriers. Finally, we washed the uncured resin with anhydrous alcohol and fine μPADs were obtained. The resolution of the fabricated hydrophilic channels was 367±20μm, with a between-channel hydrophobic barrier of 400±21μm. To verify this method's performance, we fabricated μPADs with DMPC for quantitative analysis of nitrite ion. This new method represents a leap forward in terms of time saved. Since all hydrophobic barriers are cured at a time, the fabrication process can be completed in only two minutes, no matter how complex the patterns are. Compared to the widely used fabrication method of μPADs, wax printing, DMPC provides an alternative way to fabricate μPAD with different hydrophobic barriers materials, which provides the

possibility of designing different μPADs according to the application environments.

1. Introduction

μPADs provide a minimized scale for laboratory and require only a small amount of reagent. μPADs have many advantages, since they are inexpensive as well as easy to process, carry, and dispose of. Therefore, they play an important role in medical diagnosis, food analysis, and environmental monitoring [1-2]. Many studies have explored fabrication techniques for μPADs, such as photolithography [3-5], inkjet printing [6-8], wax printing [9-11], wax screen-printing [12, 13], wax dipping [14], wax stamping [15-17], plasma treatment [18], direct writing of PDMS [19], paper cutting [20,21] and flexographic printing[22].

Whitesides and colleagues used the SU-8 photoresist as hydrophobic material [3] to form hydrophobic barriers and hydrophilic channels on the paper by exposing to the UV light under a mask cover. This method could acquire a high resolution (200μm); however, it requires a high cost and a series of complicated processing steps. Ade, et al. [6-7] developed an inkjet printing method to fabricate paper-based microfluidic devices called inkjet etching. These were done with a single printing apparatus, and μPADs can be fabricated with a resolution of 560μm (hydrophilic channels). Furthermore, the necessary reagents for colorimetric analytical assays can be printed with an inkjet printing device. This method is suitable for mass production; however, inkjet printers should be modified and the ink should be carefully designed to avoid blocking the printer nozzle.

Lu, et al. [9-10] and Carrilho, et al. [11] fabricated paper-based microfluidic devices with wax printing in a two-step process. First, the printer produced patterns of solid wax on the surface of the paper, and then the hot plate melts wax on the paper. Hydrophobic barriers and hydrophilic channels are created when the wax penetrates the paper. Hydrophilic channels can be fabricated with a resolution of 561±45μm. This simple method can support high-volume manufacturing, and is widely used in current μPAD fabrication.

Other μPADs fabrication method based on wax have also been developed, such as wax screen printing [12, 13], wax dipping [14] and wax stamping [15-17]. In wax screen printing [12, 13], the filter paper is covered by the patterned screen and the solid wax is rubbed through the screen. The printed wax is then melted into the paper to form hydrophobic barriers using a hot plate. However, this method cannot achieve high accuracy. The minimum widths of the hydrophilic channel and hydrophobic barrier are 600μm and 1300μm, respectively. In wax dipping, a metal mold is used as a mask to transfer the designed pattern onto paper by dipping this assembly stamp and paper into melted wax [14]. As for wax stamping, a hot stamp with a desired pattern is used to melt wax from the wax paper [15-17]. Since the melt wax can be spread in the paper, it is difficult to control the channel and barrier sizes of μPADs with wax methods.

Shen, et al. developed a μPAD fabrication methods based on plasma etching [18]. First, they immersed the filter paper into AKD solution. Then the immersed paper was air-dried. The paper became totally hydrophobic after being heated at 100℃ for 5

minutes. With the help of a patterned metal mask, the plasma treatment made the uncovered area hydrophilic, forming hydrophobic barriers and hydrophilic channels. Other methods, such as direct writing with a modified desktop plotter [19] and mechanical cutting [20, 21], can also be used for rapid fabrication μPADs. However, the resolution is limited, so that μPADs fabricated with these methods are better suited for qualitative rather than quantitative work.

In the majority of these μPADs fabrication approaches, a metal or quartz mask is commonly used, such as in photolithography [3], wax screen-printing [12], wax stamping [15] and plasma treatment [18], which define μPAD resolution. The manufacturing and time costs of this kind of mask are fairly high. Furthermore, the processed mask can be used to make only one type of μPAD. If the mask can be allowed dynamic change with a computer according to the desired channel pattern, fabrication cost can be greatly reduced.

SL 3DP was developed by 3D Systems as the first commercially available 3DP in 1986 [23], and is also called a stereolithography apparatus (SLA). In a typical SL 3DP process, a laser beam is controlled to draw a pattern, dot-by-dot, on the UV resin. Then the structures are built from the bottom up from a support platform that rests just below the resin surface. However, dot-by-dot fabrication is very time-consuming. Thus, a rapid SL fabrication method with a dynamic mask to cure a layer of UV resin at one time was proposed [24-27]. Two commonly-used instruments to generate dynamic masks are the liquid crystal device (LCD) [24] and digital light projection (DLP) [25-27]. Dynamic masks greatly reduce printing times, since only the layer

thickness and required exposure time in the XY plane are determinants, and not size. Since commercial SLA is very expensive, some types of open source desktop SL 3DP based on dynamic masks have been developed that are low-cost and easy to assemble or buy. Two typical open source desktop SL 3DPs are B9Creat [28] and Form1 [29], and can be purchased for less than $2,000. Since curing UV resin with a dynamic mask is rapid and the desktop SL 3DP is low-cost, we used the desktop SL 3DP to fabricate μPADs in order to lower costs, and improve resolution and speed.

2. Materials and methods

2.1 Materials

In this study, we used a UV curable resin (HTU-3928, Suzhou Lion Materials Co., Ltd., Suzhou, China) as the hydrophobization agent. Whatman No.1 was used as the filter paper, and anhydrous alcohol was used to clean out the extra uncured resin. The translucent membrane (7 inch HD film) was purchased from Amperor Electronics Co., Ltd. (Shenzhen, China) A standard solution of $NaNO_2$ (GBW(E)080223, Beijing Aikeyingchuang Biotechnology Co., Ltd., Beijing, China) and an indicator solution for NO_2^- were used to test the fabricated μPADs' applicability. Other chemicals and materials were all obtained from the Zhejiang University Supplies Center. The desktop SL 3DP with LCD as the dynamic mask for UV-pattern exposure was self-designed and self-manufactured according to the description for the open source desktop SL 3DP. A UV LED, 100W, was used to provide the UV light with a wavelength of 395-400nm and luminous flux of 100-200lm, purchased from Xinyuan

Optical-Electro co., Ltd. (Shenzhen, China). A free software called Creation Workshop Alpha 1 [30] was used to control the LCD and generate dynamic mask. The SL 3DP printer used in our experiments is almost the same with B9Creat or Form1, with a difference of dynamic mask generation, B9Creat or Form1 usually use the digital light projection (DLP), while we use liquid crystal device (LCD), detailed discussion about the dynamic mask based on LCD can be found in ref 31. Some information about the design of LCD base 3D printer can be found in ref 32-33, and of course, the researchers can also directly use our design in the following.

2.2 Fabrication of a paper-based microfluidic device

The fabrication process for the μPADs in this study is shown in Figure 1. Filter paper was cut into appropriate sizes and immersed in UV resin for 5 seconds. After the UV resin penetrated the paper completely, the UV resin-covered filter paper was placed on a thin translucent membrane with a round barrier. The filter paper on the translucent membrane was flat with no air bladder between them, to aid in appropriate formation of the channel. The translucent membrane was then placed on an LCD screen controlled by a computer. When voltage is applied to the liquid crystal molecule, the molecule tends to untwist so light can be pass through the LCD selectively. A UV LED light source is fixed just below the LCD screen. A 62mm×55mm scale convex lens whose focal length is 200mm is fixed upon the LED light. The Fresnel lens is placed between the LCD and the UV light to make the divergent light become parallel with a size of 7-inch and a focal length of 185mm. The LCD screen forms a mask of the designed channel pattern through computer

control. The detailed structure of the 2D optics (Dynamic mask) is shown in Figure 2 and a 7-inch LCD screen with a resolution of 1280×800 DPI used in our experiments. If the researchers of μPADs don't want to buy a desktop SL 3DP, they can assemble a cheaper and a portable dynamic mask according to our design as an alternative, which will only cost less $1000. The UV-light then exposes the masked filter paper for 15 seconds. Next, the filter paper is turned upside-down and exposed to UV-light for 25 seconds. This ensures that the solution won't diffuse in the fabricated μPADs. When it is removed from the translucent membranes, the cured filter paper is rinsed with anhydrous alcohol and air-dried for 60 seconds to be ready for use. The time cost of every step is shown in Table 1 and we can find that the whole process just need about two minutes.

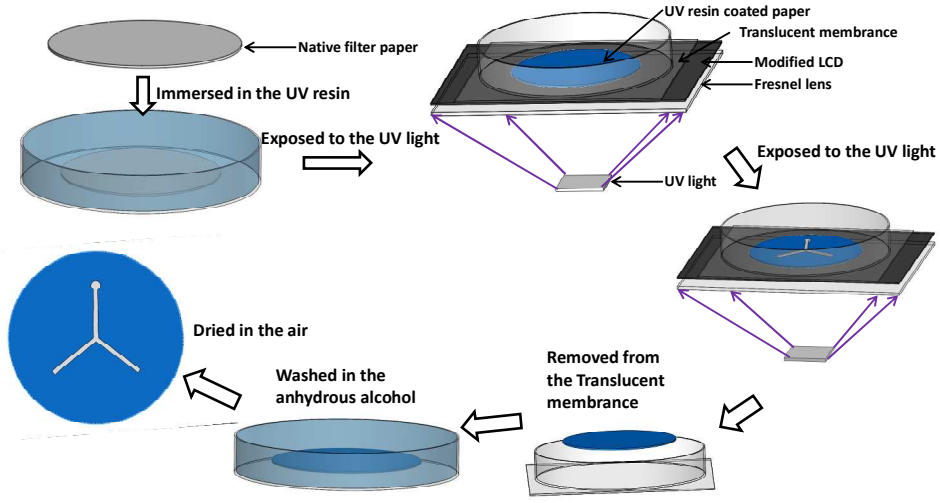

Figure 1 Fabrication process of μPADs with a dynamic mask

Table 1 Time cost of every step

Immersed	Attach	Front exposure	Second attach	Back exposure	Rinsing and drying	Total
5s	10s	15s	5s	25s	60s	120s

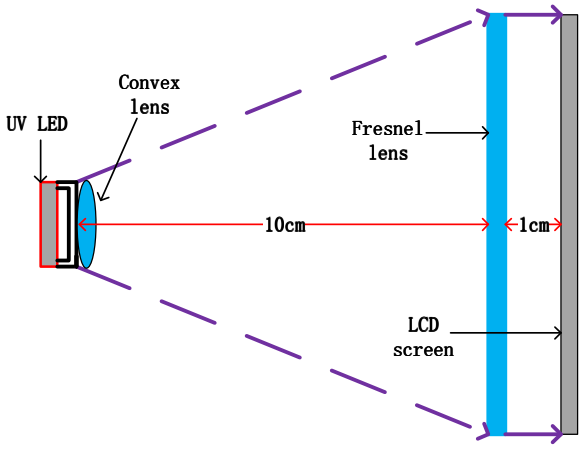

Figure 2 Detailed structure of the dynamic mask based on LCD

2.3 Assay of nitrite with the fabricated μPADs

We used the new method to fabricate the μPAD with eight detection zones for the NO_2^- assay. First, 0.04 mL NO_2^- indicator solution was placed into the central zone the bigger circle in the middle. When the indicator solution completely penetrated the detection zones, 0.01mL portions of standard solutions and the prepared sample solution were individually placed into the detection zones. After the color reaction was completely developed, the μPAD was photographed. The photo was converted to grayscale with Adobe Photoshop CS5. The curve reflected the relationship of the measured gray intensities. The standard concentration was constructed with the collected data. The concentration of the sample solution was read against the curve. The detection result was compared to the real concentration to verify the effect.

3. Results and discussion

3.1 Formation of hydrophilic-hydrophobic patterns

In this study, the hydrophilic-hydrophobic pattern production process was

divided into three steps. First, the filter paper was in UV resin for 5 seconds. Next, one side of the filter paper covered with UV resin was selectively hydrophobized by curing the UV resin. Then the other side of the filter paper was completely hydrophobized. The effects in the third step are very important. Since the filter paper is opaque, the back side of the filter paper cannot completely cure. Thus, solution dropped on the paper would diffuse in an uncontrolled manner. Therefore, the translucent membrane between the filter paper and the LCD screen should be specially processed. Since the UV resin would stick to the translucent membrane after being exposed to the UV light, it would be inconvenient to remove the cured filter paper.

Therefore, for an accurate experimental result, one side of the translucent membrane should be covered with a thin layer of resist material to prevent cured UV resin from adhering to it. We adapted the PET protective film in this manner for this study. PET protective film has a layer of glue on one side to eliminate sticking when it is exposed to UV light. Furthermore, PET film has high light transmittance of 90%. All of these characteristics make PET protective film the best choice for a translucent membrane. Anhydrous alcohol can be used to dissolve the liquid UV resin. When the exposed paper was rinsed with anhydrous alcohol, the cured UV resin remain in its original form, while the liquid UV resin in the paper would dissolve, and this area of the paper would turn hydrophilic.

The exposure process includes two steps: the front side (patterned side) exposure and the back side exposure. The front side was exposed to the UV light under the

mask to get the needed pattern. The back side was exposed to the UV light totally to make sure the solution won't diffuse in the channels. To demonstrate the significant effect of the back side exposure, a comparative experiment was performed, as shown in Figure 3. The dye flow was observed in two μPADs with Y shaped channels which were made with and without back side exposure respectively. As shown in the Figure 3a, the dye in the channel diffused to other area if the μPAD fabricated without back side exposure. The cross-sectional images of the channel under the microscope showed the same result, as shown in Figure 3b. However if the back side exposure was used, the dye only flowed along the channel, Figure 3c, and the cross-sectional images of the channel under the microscope showed that only the channel was hydrophilic, Figure 3d. The black line in Figure 3a and Figure 3c shows the location of the cross-sectional area.

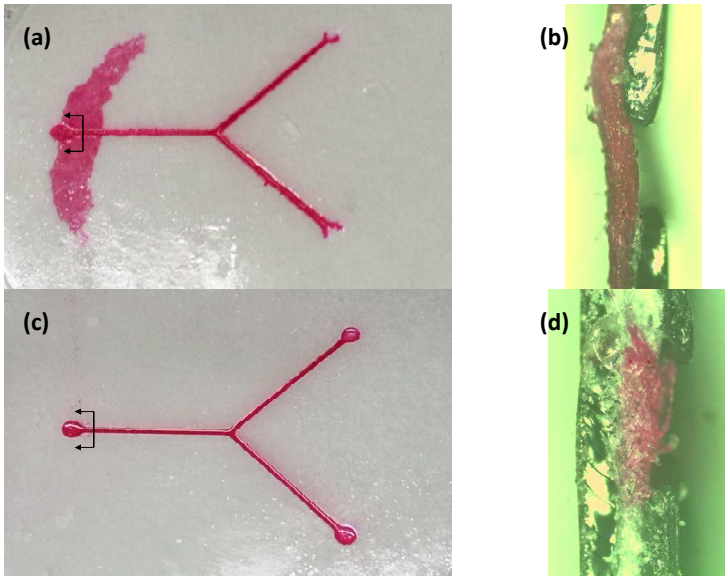

Figure 3 Comparative experiment of with and without back side exposure. (a) Dye diffused in μPAD fabricated without back side exposure and (b) its cross-sectional image of the channel under the microscope (50X). (c) Dye diffused in μPAD fabricated with back side exposure and (d) its cross-sectional image of the channel under the microscope (50X).

3.2 Optimization of exposure time

Because of the scattering effect when UV light passes through the LCD screen, the exposure time for both sides of the immersed filter paper affect the quality of the μPADs. Therefore, this study examined optimal exposure time. With a same channel pattern, a width of 500μm, the immersed paper was exposed to the UV light in different times to evaluate the influence of the exposure time of both sides. First, the patterned side was exposed to the UV light between 5s and 25s. Tests revealed that the cured hydrophilic-hydrophobic pattern thins as the exposure time lengthens. As the curve shows in Figure 4a, an optimal curing result was achieved at 15s, the channel width is near 500μm, the designed channel size, at this time. Second, with a 15s front exposure time, the back of the patterned paper was completely exposed to UV light between 5s and 45s. As shown in Figure 4b, the diffusion rate of dye reached an average level at 25s. If the exposure time of back side was less than 15s, the resin wasn't completely solidified and the phenomena like Figure.3a was still happen. If the time was too long, large than 30s, some resin filled in the channel and it was hard to control the channel quality. Thus, the optimal exposure time for the back side was chose at 25s.

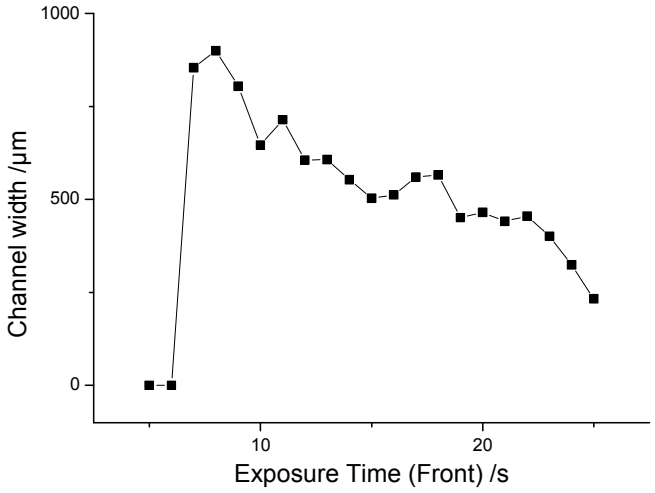

(a)

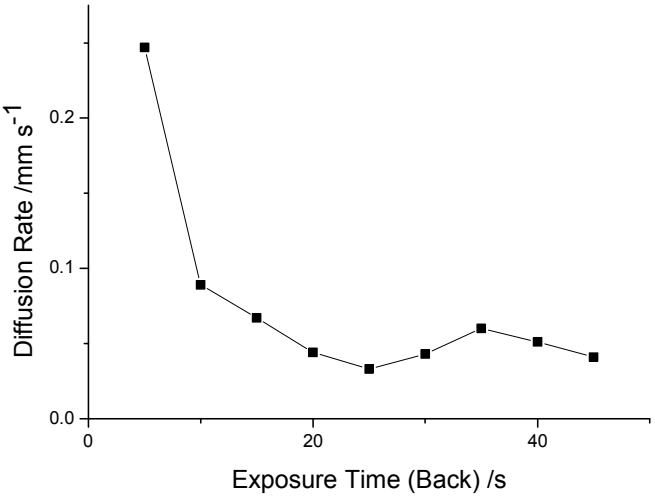

(b)

Figure 4 Optimal exposure time: (a) Curve of the relationship between the channel width and the front exposure time; (b) Curves on the effect of the back exposure time on diffusion rate.

3.3 Resolution of DMPC

The resolution of hydrophilic channels and hydrophobic barriers was evaluated in two aspects: static and dynamic. Here, we used static resolution to describe how the minimal width of the hydrophilic channel and the hydrophobic barrier are preserved when the μPAD is immersed in dye. The minimal width of the hydrophilic channel

with complete submersion is defined as the static resolution of the hydrophilic channel. Conversely, the minimal width of the hydrophobic barrier without submersion is defined as the static resolution of the hydrophobic barrier. The term "dynamic resolution" describes a situation where the minimal width of the hydrophilic channel and hydrophobic are preserved in the analysis. The minimal width of the hydrophilic channel that can be retained for the analysis is defined as the dynamic resolution of the hydrophilic channel. Conversely, the minimal width of the hydrophobic barrier that can be isolated in a sample in the analysis is defined as the dynamic resolution of the hydrophobic barrier. The widths of hydrophilic channels and hydrophobic barriers were measured with a digital microscope (KEYENCE). The dynamic resolution of the hydrophilic, hydrophobic pattern on filter paper was measured using the method described in Ref 31.

For both aspects, DMPC was used to fabricate a series of hydrophilic and hydrophobic channels with a small gradient from largest to smallest. As shown in Figure 5, the static resolution for hydrophilic channels was 332±17μm, and that for the between-channel hydrophobic barrier was 349±18μm. As shown in Figure 6, the dynamic resolution for hydrophilic channels was 367±20μm, and that for the between-channel hydrophobic barrier was 400±21μm. In contrast to traditional fabricating methods such as wax printing, DMPC showed good performance.

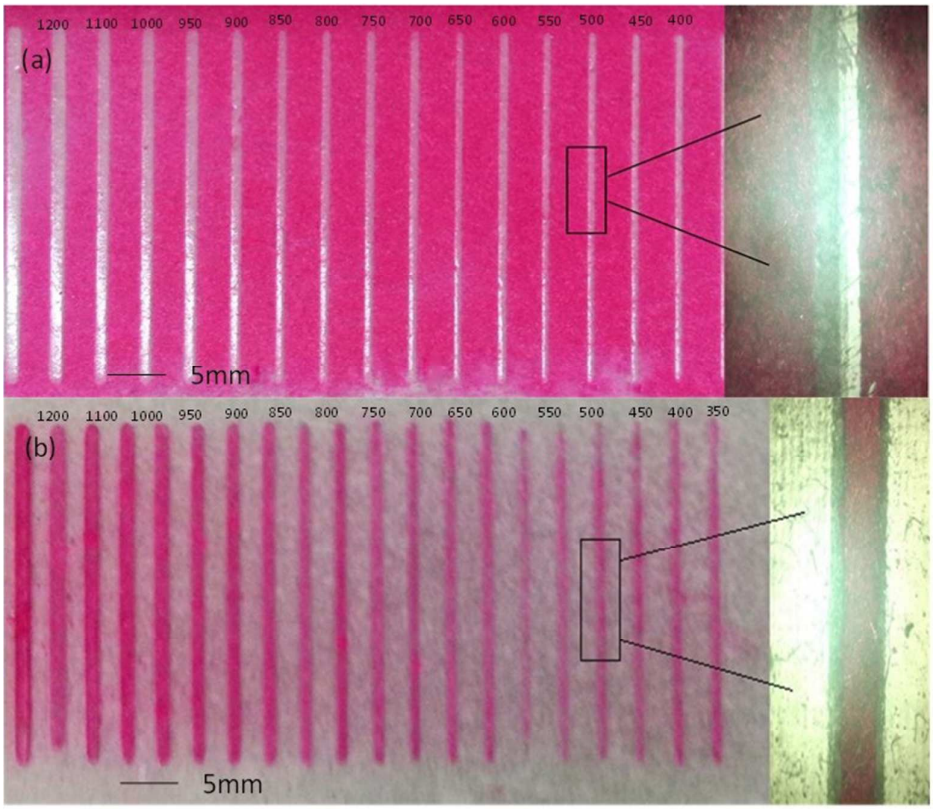

Figure 5 Static resolution of hydrophilic−hydrophobic contrast on the μPADs prepared with the new method. Part a shows the resolution of the hydrophilic channels and the channel's image under the microscope (100X). Part b shows the resolution of the hydrophobic barriers and the barrier's image under the microscope (100X).

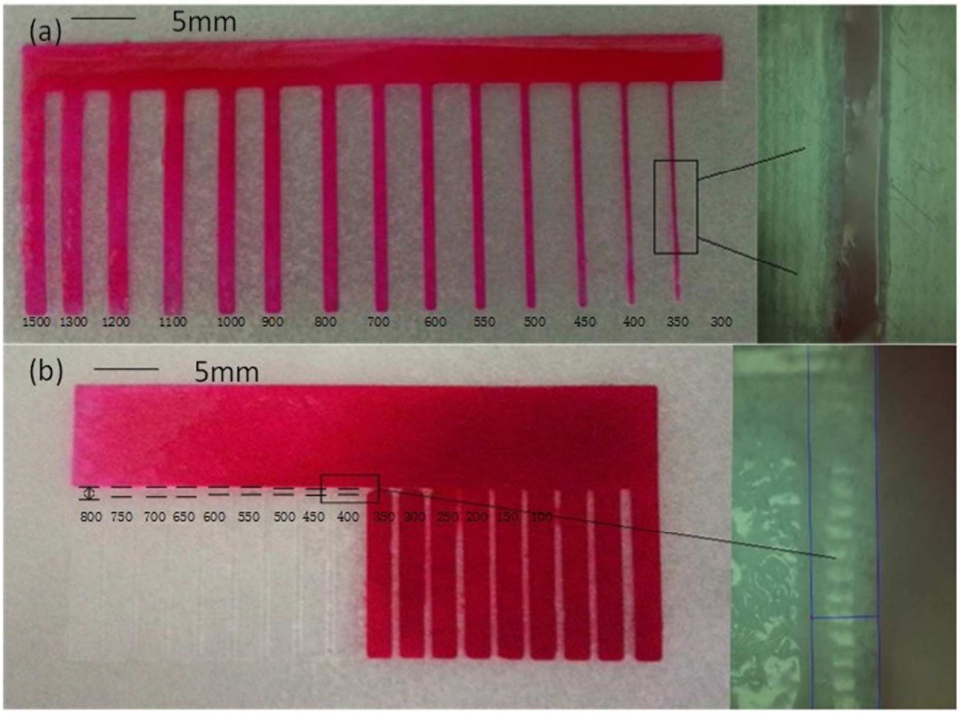

Figure 6 Dynamic resolution of hydrophilic−hydrophobic contrast on μPADs prepared with the new method. Part A shows the resolution of the hydrophilic channels and the channel's image under the microscope (100X). Part B shows the resolution of the hydrophobic barriers and the barrier's image under the microscope (100X).

3.4 Complex pattern fabrication

In this study, two μPADs with complicated channel patterns were fabricated to show the capability of this method. This method allowed successful fabrication of patterns from a Chinese map (Figure 7a), the logo of Zhejiang University (Figure 7b), and the time-lapse images of how the dye diffused in the channel of Chinese map (Figure 7c). The complicated hydrophilic-hydrophobic channels were intact, and the dye diffused to every corner of the hydrophilic channels. The outstanding performance of this method indicates its promise for application.

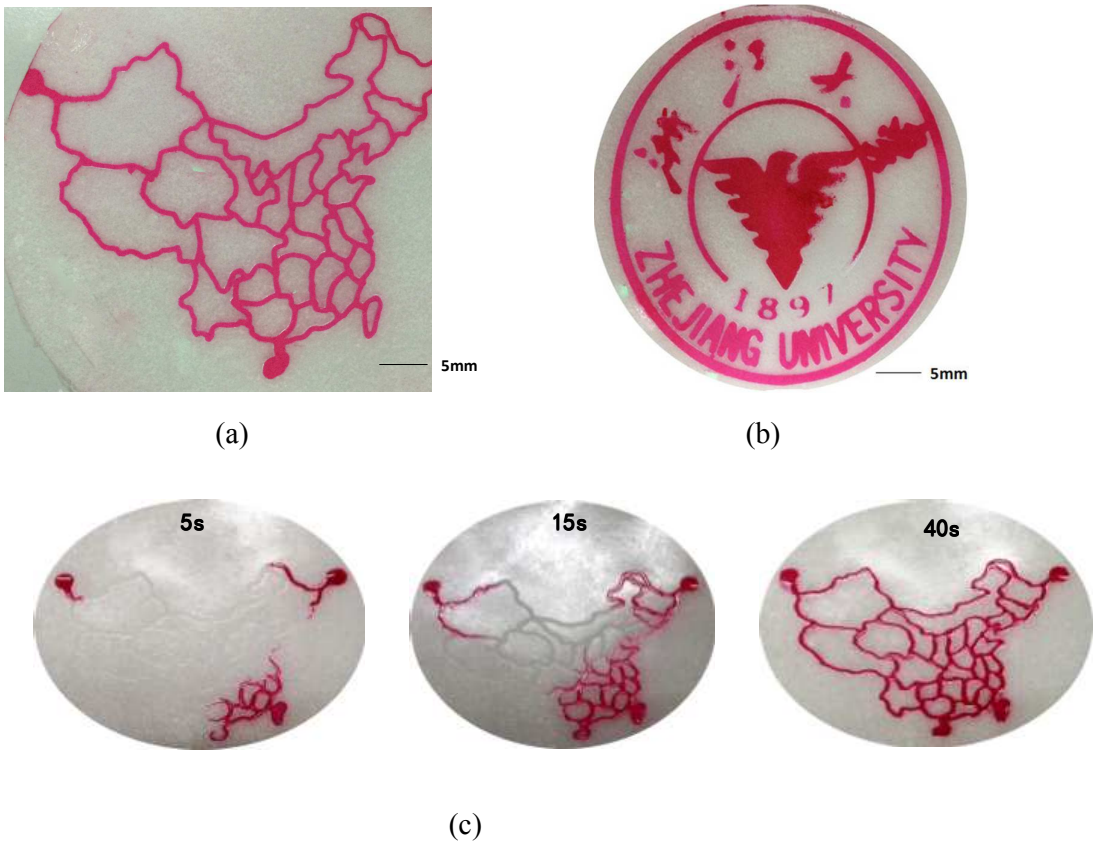

Figure 7 μPADs with complicated patterns, (a) map of China; (b) logo of Zhejiang University; (c)

Time-lapse images of the dye diffused in the channel.

3.5 Assay of nitrite concentration test

To demonstrate the μPAD's practicability, a μPAD fabricated with DMPC was evaluated using quantitative analysis as a case study. The μPAD had eight detection zones. When all detection zones were filled with an NO_2^- indicator solution, 7 were dropped with standard nitrite solution. The last one was dropped with the determined solution, with a known concentration. The nitrite concentration of each sample is listed in Table 2. As shown in Figure 8b, the 1-7 detection zones reflected the color reaction. The collected photo was turned into grayscale and data was collected and listed in Table 2. A curve that reflect the relationship between the nitrite concentration and the corresponding gray intensity was obtained by fitting at least squares principle. As shown in Figure 8a, the curve was constructed and the regression equation is $y = 3.4978x + 57.868$ and the R^2 is 0.9282, which shows the line is fitted well. According to the equation, the gray intensity is 84 and its corresponding testing result is 7.47μg/L. Results show that, compared to the real concentration of 7.5μg/L, the designed μPAD demonstrates capability for quantitative analysis.

Table 2 Nitrite concentration of sample 1-7 and their corresponding gray intensity

Sample	1	2	3	4	5	6	7
Gray Intensity	90	86	81	78	67	63	59
Nitrite Concentration μg/L	10	8	6	4	3	2	1

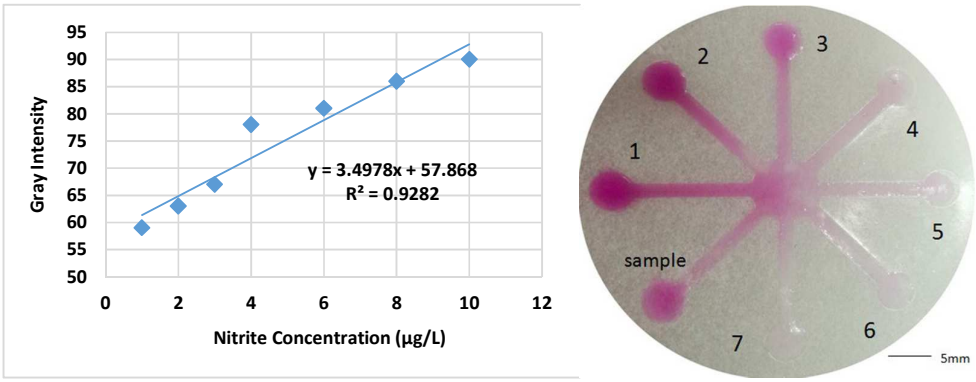

(a) (b)

Figure 8 Colorimetric assay of nitrite via color-reaction by using μPAD: (a) Curve for nitrite ion; (b) Image of the testing μPAD

3.6 Discussion

Compared to the widely used fabrication method of μPADs, wax printing, DMPC provides an alternative way to fabricate μPADs with different materials, different equipment and good resolution. Firstly, DMPC has multiple materials that can be used as hydrophobic barriers, any type of photo curing resin can be used to fabricate μPADs, which means that design of specially used μPADs according to the application environments becomes possible. For example, if the temperature of analytical chemistry field is high over 50ºC, μPADs fabricated by wax printing cannot be used, as the wax barriers will melt. Or sometimes we hope μPADs can be bended and folded to form 3D structures for acquiring better analytical performance, wax printing is also not suitable, as the wax is brittle. Secondly, researchers can directly buy a desktop SL 3DP to fabricate μPADs. Now desktop 3DP is developed rapidly and a big drop of price will be expected in the near future, as this may become as popular as the personal computer. In this paper, we also provided the detailed design of one kind dynamic mask, key part of a desktop SL 3DP, as an alternative solution,

so researchers can assemble one with a more low cost and fabricate μPADs with this. At last, the resolution of DMPC is determined by the resolution of dynamic mask, in this paper, the dot pitches of LCD. So with development of integrated circuit industry, LCD with small dot pitches will be fabricated, and the resolution of DMPC will also be improved.

4. Conclusions

DMPC is a simple, rapid method for fabrication of μPADs, with a large potential to become a mass μPADs fabrication method. This method takes full advantage of UV resin's characteristics. The cured resin is hydrophobic and solid, which can form hydrophobic barriers. With the dynamic mask, a new patterned, virtual mask can be easily obtained with a computer. In this way, a new patterned μPAD can be fabricated in a few minutes from design to product, aiding analysts by shortening the time needed for scientific research to a large degree. Good resolution of the hydrophilic-hydrophobic channels was obtained. The smallest hydrophilic channel width was 332±17μm, which is sufficient for the assay request. The assay of nitrite on the fabricated μPAD also shows its capability.

Acknowledgments

This paper was sponsored by the Science Fund for Creative Research Groups of the National Natural Science Foundation of China (no. 51221004), the National Natural Science Foundation of China (no. 51375440), Fundamental Research Funds for the Central Universities (no. 2013QNA4007), and Zhejiang Provincial Natural Science Foundation of China (no. LY12E05018).

References

1 Martinez A W, Phillips S T, Whitesides G M, et al. Diagnostics for the developing world: microfluidic paper-based analytical devices[J]. Analytical chemistry, 2009, 82(1): 3-10.

2 Li X, Ballerini D R, Shen W. A perspective on paper-based microfluidics: current status and future trends[J]. Biomicrofluidics, 2012, 6(1): 011301.
3 Martinez A W, Phillips S T, Butte M J, et al. Patterned paper as a platform for inexpensive, low‐volume, portable bioassays[J]. Angewandte Chemie International Edition, 2007, 46(8): 1318-1320.
4 Haller P D, Flowers C A, Gupta M. Three-dimensional patterning of porous materials using vapor phase polymerization[J]. Soft Matter, 2011, 7(6): 2428-2432.
5 He Q, Ma C, Hu X, et al. Method for fabrication of paper-based microfluidic devices by alkylsilane self-assembling and UV/O3-patterning[J]. Analytical chemistry, 2013, 85(3): 1327-1331.
6 Abe K, Suzuki K, Citterio D. Inkjet-printed microfluidic multianalyte chemical sensing paper[J]. Analytical chemistry, 2008, 80(18): 6928-6934.
7 Abe K, Kotera K, Suzuki K, et al. Inkjet-printed paperfluidic immuno-chemical sensing device[J]. Analytical and bioanalytical chemistry, 2010, 398(2): 885-893.
8 Li X, Tian J, Garnier G, et al. Fabrication of paper-based microfluidic sensors by printing[J]. Colloids and Surfaces B: Biointerfaces, 2010, 76(2): 564-570.
9 Lu Y, Shi W, Jiang L, et al. Rapid prototyping of paper‐based microfluidics with wax for low‐cost, portable bioassay[J]. Electrophoresis, 2009, 30(9): 1497-1500.
10 Lu Y, Shi W, Qin J, et al. Fabrication and characterization of paper-based microfluidics prepared in nitrocellulose membrane by wax printing[J]. Analytical chemistry, 2009, 82(1): 329-335.
11 Carrilho E, Martinez A W, Whitesides G M. Understanding wax printing: a simple micropatterning process for paper-based microfluidics[J]. Analytical chemistry, 2009, 81(16): 7091-7095.
12 Dungchai W, Chailapakul O, Henry C S. A low-cost, simple, and rapid fabrication method for paper-based microfluidics using wax screen-printing[J]. Analyst, 2011, 136(1): 77-82.
13 Dungchai W, Chailapakul O, Henry C S. Electrochemical detection for paper-based microfluidics[J]. Analytical chemistry, 2009, 81(14): 5821-5826.
14 Songjaroen T, Dungchai W, Chailapakul O, et al. Novel, simple and low-cost alternative method for fabrication of paper-based microfluidics by wax dipping[J]. Talanta, 2011, 85(5): 2587-2593.
15 Curto V F, Lopez-Ruiz N, Capitan-Vallvey L F, et al. Fast prototyping of paper-based microfluidic devices by contact stamping using indelible ink[J]. RSC Advances, 2013, 3(41): 18811-18816.
16 Zhang Y, Zhou C, Nie J, et al. Equipment-free quantitative measurement for microfluidic paper-based analytical devices fabricated using the principles of movable-type printing[J]. Analytical chemistry, 2014, 86(4): 2005-2012.
17 Garcia D T P, Cardoso T M G, Garcia C D, et al. A handheld stamping process to fabricate microfluidic paper-based analytical devices with chemically modified surface for clinical assays[J]. RSC Advances, 2014, 4(71): 37637-37644.
18 Li X, Tian J, Nguyen T, et al. Paper-based microfluidic devices by plasma treatment[J]. Analytical chemistry, 2008, 80(23): 9131-9134.
19 Bruzewicz D A, Reches M, Whitesides G M. Low-cost printing of poly (dimethylsiloxane)

barriers to define microchannels in paper[J]. Analytical chemistry, 2008, 80(9): 3387-3392.

20 Chitnis G, Ding Z, Chang C L, et al. Laser-treated hydrophobic paper: an inexpensive microfluidic platform[J]. Lab on a Chip, 2011, 11(6): 1161-1165.

21 Fenton E M, Mascarenas M R, López G P, et al. Multiplex lateral-flow test strips fabricated by two-dimensional shaping[J]. ACS applied materials & interfaces, 2008, 1(1): 124-129.

22 Olkkonen J, Lehtinen K, Erho T. Flexographically printed fluidic structures in paper[J]. Analytical chemistry, 2010, 82(24): 10246-10250.

23 Melchels F P W, Feijen J, Grijpma D W. A review on stereolithography and its applications in biomedical engineering[J]. Biomaterials, 2010, 31(24): 6121-6130.

24 Itoga K, Yamato M, Kobayashi J, et al. Cell micropatterning using photopolymerization with a liquid crystal device commercial projector[J]. Biomaterials, 2004, 25(11): 2047-2053. LCD

25 Sun C, Fang N, Wu D M, et al. Projection micro-stereolithography using digital micro-mirror dynamic mask[J]. Sensors and Actuators A: Physical, 2005, 121(1): 113-120.

26 Lu Y, Mapili G, Suhali G, et al. A digital micro‐mirror device‐based system for the microfabrication of complex, spatially patterned tissue engineering scaffolds[J]. Journal of Biomedical Materials Research Part A, 2006, 77(2): 396-405.

27 Pan Y, Zhou C, Chen Y. A fast mask projection Stereolithography process for fabricating digital models in minutes[J]. Journal of Manufacturing Science and Engineering, 2012, 134(5): 051011.

28 B9 Creations, B9 Creator, http://b9creator.com/, (date unknown) (Date of access: 30/08/2014)

29 Formlabs: Form1+ High-Resolution 3D Printing, http://formlabs.com/en/products/form-1-plus/, (2014) (Date of access: 30/08/2014).

30 PacManFan: Creation Workshop - SLA / FDM Slicer and Controller, http://www.thingiverse.com/thing:40778, (2013) (Date of access: 8/01/2013).

31 Bertsch A, Zissi S, Jezequel J Y, et al. Microstereophotolithography using a liquid crystal display as dynamic mask-generator[J]. Microsystem Technologies, 1997, 3(2): 42-47.

32 http://www.lcd3dprinter.com/

33 http://www.buildyourownsla.com/